Environmental Pollution 337 (2023) 122550

Contents lists available at ScienceDirect

Environmental Pollution

journal homepage: www.elsevier.com/locate/envpol

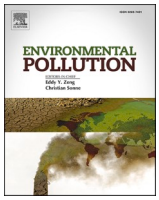

Cellular and bioenergetic effects of polystyrene microplastic in function of cell type, differentiation status and post-exposure time☆

Miao Peng [a,b,*], Maaike Vercauteren [a,b], Charlotte Grootaert [c], Andreja Rajkovic [c], Nico Boon [d], Colin Janssen [a,b], Jana Asselman [a,b]

[a] Laboratory of Environmental Toxicology and Aquatic Ecology, Faculty of Bioscience Engineering, Ghent University, Coupure Links 653, 9000, Ghent, Belgium
[b] Blue Growth Research Lab, Ghent University, Wetenschapspark 1, 8400, Oostende, Belgium
[c] Department of Food Technology, Safety and Health, Faculty of Bioscience Engineering, Ghent University, Coupure Links 653, 9000, Ghent, Belgium
[d] Center for Microbial Technology and Ecology (CMET), Faculty of Bioscience Engineering, Ghent University, Coupure Links 653, 9000, Ghent, Belgium

ARTICLE INFO

Keywords:
Microplastics
Long-term impacts
Bioenergetic effects
Cell differentiation
Low particle concentrations

ABSTRACT

The ubiquity of microplastics (MPs) in food sources and personal care products increasingly raises concerns on human health. However, little is known about the duration of the effects of MPs and whether effects depend on cellular differentiation status. Herein, cellular and bioenergetic effects of MPs in different exposure scenarios on four types of human cell lines derived from lung (A549 and BEAS-2B), colon (Caco-2) and liver (HepG2) were investigated. These cell lines are models for the major exposure routes in the body (inhalation, ingestion and physiological transport through the liver by the portal vein). To this aim, different scenarios were implemented by exposing undifferentiated and differentiated cells to single dosing of 2-μm polystyrene (PS) (10^2-10^5 particles/mL) for 48 h and 12 days. The undifferentiated Caco-2 cells with short exposure (48 h) showed the highest uptake rate of PS yet without significant cellular and mitochondrial responses. The biological effects, with the exception of ROS production, were not influenced by differentiation states of A549 and Caco-2 cells although differentiated cells showed much weaker ability to internalize PS. However, PS had significantly long-term impacts on cellular and mitochondrial functions even after the initial exposure period. In particular, Caco-2 cells that were post-exposed for 12 days after single PS dosing suffered higher oxidative stress and exhibited mitochondrial dysfunction than that for short exposure. Correspondingly, we observed that PS particles still remained in cell membrane and even in nuclei with high retention rate by 14-d post exposure during which metabolism and exchange of internalization and release occurred in cells. This indicates PS could induce chronic stress and even harmful effects on human cells after single intake that persists for a long time. This study paves the way for assessing the influence of PS on human health at low particle concentrations and with multiple exposure scenarios.

1. Introduction

Plastic products (such as food contact materials, food and drinking packaging and synthetic clothing) are widely used in our daily life. These can unintentionally release micro-/nanoplastics (MNPLs) due to weathering or friction processes (hydrolysis, UV photodegradation and mechanical abrasion) occurring ubiquitously in our living environment (Alimi et al., 2018; Dalla Fontana et al., 2020; Fadare et al., 2020). MNPLs are also intentionally added components of products, such as exfoliating facial scrubs, toothpastes and resin pellets (Hernandez et al., 2017) with the potential to accumulate in the food chain (Sana et al., 2020). At present, MNPLs have been detected in various food and beverages for human consumption such as drinking water, seafood, honey, table salt, milk and even in both in- and outdoor air (Elkhatib and Oyanedel-Craver, 2020; Gasperi et al., 2018; Kutralam-Muniasamy et al., 2020; Liebezeit and Liebezeit, 2013; Van Cauwenberghe and Janssen, 2014; Yang et al., 2015). Thus, MNPLs are ubiquitous in our environment and pose potential threats to human health through inhalation or ingestion.

Human biomonitoring studies have detected microplastics (MPs)

☆ This paper has been recommended for acceptance by Maria Cristina Fossi.

* Corresponding author. Faculty of Bioscience Engineering, Ghent University, Coupure Links 653, 9000, Ghent, Belgium.
E-mail address: miao.peng@ugent.be (M. Peng).

https://doi.org/10.1016/j.envpol.2023.122550
Received 5 July 2023; Received in revised form 21 August 2023; Accepted 12 September 2023
Available online 15 September 2023

with the size of 50–500 μm in human stool (Schwabl et al., 2019). Furthermore, smaller MPs particles (less than 10 μm) are capable to cross human biological barriers and potentially transfer to organs and tissues, which was confirmed by the observation of MNPLs in human placentas, lung tissue and blood (Amato-Lourenço et al., 2021; Bruinink et al., 2015; Leslie et al., 2022; Ragusa et al., 2021). In terms of effect studies, a substantial number of studies (see Table S1 in supporting information) have focused on the toxicological assessment of MNPLs on human health, primarily using cell lines derived from colon (Caco-2, HT-29), lung (A549, BEAS-2B) and liver (HepG2, HL-7702) since those organs can come into contact with MNPLs after ingestion or inhalation. From previous research, it is clear that MNPLs can enter human cells (including nuclei, lysosomes and cytoplasm) and potentially trigger toxicity at high concentrations (Bonanomi et al., 2022; Cortés et al., 2020; Liu et al., 2021). For instance, it is reported that the cell viability of Caco-2 and A549 cells showed a significant decrease at a high concentration of polyethylene (PE) (6.2 μm, 1000 μg/mL, 8.71×10^6 particles/mL), and this high dose significantly increased ROS production in U937 and THP-1 cells (Gautam et al., 2022). Furthermore, one study conducted proteomic and metabolomic analysis and found 785 proteins and 17 metabolites with altered levels when HKC and HL-7702 cells were exposed to high polystyrene (PS) concentration (80 nm, 100 μg/mL, 3.55×10^{11} particles/mL) (Wang et al., 2022). Most studies reported exposure levels in mass concentration (μg/mL, see Table S1). However, for biological effects, particle number concentration (particles/mL) is likely to be more informative since it is the individual particle that will interact with cells (Connors et al., 2017). After converting mass concentrations into particle concentrations in the published papers, it is remarkable that the used particle concentrations, mainly ranging between 10^4 and 10^{12} particles/mL (see Table S1), are much higher than those currently documented in possible exposure concentrations for humans (no more than 10^5 particles/mL for MPs, see Table S2). Therefore, there is a mismatch between the exposure and effect studies which makes it difficult to properly assess potential risks of MPs at lower levels of exposure.

Biological effects do not solely depend on exposure concentrations, but are also a function of cell type, differentiation status, post-exposure time indicating possibly different risks at different organs and endpoints. As summarized in Table S1, current literature mainly set undifferentiated cells as exposure targets with short exposure time. In general, upon reaching confluency, cells may undergo differentiation process with significantly morphological and physiological changes during a long culture time. In that case, differentiated cells are closer to in-vivo status and reflect more physiologically relevant conditions. At this moment it is not clear whether undifferentiated or differentiated cells provide sufficiently similar models to assess in-vivo effects. Moreover, single dosing with long-term effects, nearly ignored by most studies, is an essential occasion occurring in our daily life (i.e. intake of MPs which are not immediately removed and as such exposure continues to last). Therefore, to comprehensively understand the toxicity of MPs, the effects on differentiated cells and cells with single dosing for long-term period should also be tested.

The current study aims to comprehensively evaluate biological effects of PS with concentrations close to human exposure levels (based on current exposure data) on multiple human cell lines with different differentiation status and culture time after a single dosing. To this aim, four types of human cell lines derived from colon (Caco-2), liver (HepG2) and lung (A549 and BEAS-2B) were exposed to 2-μm PS microspheres (10^2-10^5 particles/mL) with single dosing for 48 h and 12 d. We specifically selected the plastic material and cell types to match those currently used in literature to benchmark our results to previous work at higher exposure concentrations. The four chosen cell lines represent the key target organs relevant for MPs exposure via inhalation, ingestion and detoxification. PS was selected because of its wide presence in daily used products and easy control of size during material synthesis. The 2-μm plastic particles were used in our study for two reasons: 1) larger particles cannot be internalized by cells and 2) human exposure data of smaller nano-sized particles are not well validated yet, which makes it impossible to select relevant exposure concentrations (Bruinink et al., 2015; Zarus et al., 2021). The basic cellular responses or parameters were measured by biochemical assays (intracellular reactive oxygen species, mitochondrial membrane potential, sulforhodamine B and MTT assays). Mitochondrial respiration parameters and bioenergetic status, the vital indicators of cell metabolism, immunity and function, were analyzed by a Seahorse efflux analysis experiment. Flow cytometry and confocal microscopy were used to monitor dynamic processes of uptake, release and localization of PS during exposure especially for long-term period. This study is the first to systematically investigate the effects of PS in relation to cell type, differentiation status and post-exposure time under a concentration range close to reported human exposure levels. Those data could provide a first step towards comprehensive risk assessment of MPs exposure for human health and stimulate further research on real-life scenarios of MPs.

2. Materials and methods

2.1. Cell culture

The adenocarcinomic human alveolar basal epithelial cell line (A549) and adenovirus-12 SV40 transformed human bronchial epithelium cell line (BEAS-2B), available at Laboratory of Environmental Toxicology and Aquatic Ecology (GhEnToxLab, Ghent University) and deposited under Biobank number BR-42, were used. The adenocarcinomic human epithelial colon cell line (Caco-2) and adenocarcinomic human liver cell line (HepG2) were obtained from ATCC and deposited under Biobank number BB190156. We selected these cell lines as they are the classic model cells in vitro to study cytotoxicity of toxins or pollutants (Liu et al., 2020; Persoz et al., 2010). Also, they feature many in vivo pulmonary, intestinal and hepatic characteristics (Arzumanian et al., 2021; Braga et al., 2018; Persoz et al., 2012). Undifferentiated A549, BEAS-2B and HepG2 cell lines were cultured in Dulbecco's modified eagle medium (DMEM) supplemented with phenol red, 10% fetal bovine serum (FBS), 100 U/mL penicillin and 100 μg/mL streptomycin (Mohammed et al., 2018; Van Acker et al., 2020). The differentiated and undifferentiated Caco-2 cells were grown in supplemented DMEM medium, as described above, with addition of 2% nonessential amino acids (NEAA) (Liu et al., 2004; Pichardo et al., 2017). Differentiated A549 cells were cultured in F-12 Nutrient Mixture supplemented with phenol red, 10% FBS, 100 U/mL penicillin and 100 μg/mL streptomycin (Cooper et al., 2016). All culture and supplemented media were purchased from Thermo Fisher Scientific, USA. All cell lines were incubated at 37 °C, 5% CO_2 and a relative humidity of 95%–100%. Cell lines were checked daily for growth and confluence. Confluent cells were sub-cultured by 0.5% Trypsin-EDTA (Thermo Fisher Scientific, USA) and cells were split once a week with ¼ ratio. The passage numbers of all cultured cell lines were within the value of 50 during the whole research.

Differentiation of the cell lines:

- Caco-2: Caco-2 cells are able to be differentiated on 2D Transwell® plates after 21-day culture (Natoli et al., 2011). However, cells would acidify too much and start to detach from full-bottom standard culture plates used in this study after 14 days according to our previous experience with this batch of cell line (Geirnaert et al., 2017; Wu et al., 2017). It is reported that Caco-2 cells exhibited well-defined tight junctions and kept high and stable transepithelial electrical resistance (TEER) after 13-d culture, indicating they are differentiated enough (Hidalgo et al., 1989). Therefore, the maximum time to make Caco-2 cells differentiated is 14 days in our work.
- A549 & BEAS-2B: It is reported that differentiated lung cells (such as A549 cells) exhibited significant up-regulated gene expression involved in lipidogenic pathway, which induced increased lipid

production (Cooper et al., 2016; Corbière et al., 2011). Thus, to keep the same culture time as Caco-2 cells, we cultured both A549 and BEAS-2B cells (derived from lung) for 14 days and then checked differentiated status by staining lipid in Adipored assay. As shown in Fig. S5, lipid production of A549 was significantly increased after 14-days culture while BEAS-2B did not have any lipid increase with increment of culture time. Vividly, we observed lipid droplets in both A549 and BEAS-2B cells (white dots in yellow circles, see Fig. S6 and Fig. S7). The quantity of lipid droplets in A549 increased significantly after 14 days, which was much higher than that in BEAS-2B at same timeslot. Those results indicate A549 cells became differentiated while BEAS-2B cells could not be differentiated after 14 days in this culture system.

- HepG2: Unfortunately, to the best of our knowledge, HepG2 cells cannot differentiate on two-dimensional (2D) tissue culture surfaces while they would stop proliferating and differentiate to form spheroids in three-dimensional (3D) in vitro model (Ramaiahgari et al., 2014). Thus, it is not feasible to culture differentiated HepG2 cells in this work that used 2D culture flasks and well plates.

Also, the images of cultured A549 and Caco-2 cells after 12 days by light microscopy displayed well growth morphology and domes formation (Fig. S8, yellow circles) which is also a sign of differentiation reported by literature (Lever, 1979). Therefore, A549 and Caco-2 cells were selected as differentiated models for the following exposure targets and the total culture time is 14 days in this work.

2.2. Microplastics (PS)

In this study, 2-μm polystyrene (PS) microspheres were used with yellow/green fluorescence (Fluoresbrite®, Polysciences Inc.), provided as a sterile 2.5% aqueous suspension (5.68×10^9 particles/mL (P/mL)) by manufacturer. Size, shape and concentration of the PS particles in the stock solution was confirmed using scanning electron microscopy and flow cytometry (Supplementary file 2). After ultrasonic treatment (5 min) and vortex, the stock solution was continuously diluted 100 times twice with culture medium (supplemented with 100 U/mL penicillin and 100 μg/mL streptomycin) to obtain 5.68×10^5 P/mL theoretically, which was set as the highest tested concentration in this work based on the summary of the highest reported human exposure concentration (10^5 P/mL in Table S2). Lower concentrations were derived from a dilution factor of 10 from the highest concentration (5.68×10^5 P/mL). After dilutions, the expected exposure concentrations were 1.14×10^2, 1.14×10^3, 1.14×10^4, 5.68×10^4, 5.68×10^5 P/mL.

2.3. Exposure of the cells with microplastics (PS)

Schematic overview of three scenarios that mimic real-life exposure is depicted in Fig. 1. Prior to the experiment, trypsinized cell lines were detached and suspended in culture medium as described above. First, the cell suspension was diluted and seeded in 96-well plates (20000 cells per well with 200 μL medium) for the cellular assays (see below), in 24 well-plates (100000 cells per well with 1000 μL medium) for flow cytometry measurements (see below) and in a chambered coverslip with 8 wells (30000 cells per well with 300 μL medium) for confocal microscopy observations (see below). The seeding density of cells was selected based on previous literature (Chen et al., 2022). With this seeding density, cells would be at least 80% confluent after 48-h culture to guarantee they are stable and robust before PS exposure.

In order to mimic possible real-life situations, three exposure scenarios were used in this work. Scenario 1 entails the study of short exposure (48 h) of undifferentiated cells (prior to 48-h culture of seeding cells). In scenario 2, cells were first cultured until differentiation (after 12 days) and the differentiated cells were subsequently exposed to the PS with same short exposure (48 h). For scenario 3, after 48-h culture of seeding cells, confluent cells were exposed to PS once and then these exposed cells were grown for 12 days during differentiation process to investigate longer-term effects. The maximum culture time of cells was kept for 14 days in this study as cells would acidify too much and start to detach from the bottom if we culture them longer in full-bottom standard culture plates.

After PS exposure, four biochemical assays were conducted to evaluate the effects on cell viability (MTT assay aims to measure mitochondrial activity and SRB assay aims to measure protein contents), oxidative stress (ROS assay) and mitochondrial membrane potential (TMRE staining). For each PS exposure concentration, six wells with the same exposure concentration and passage number were analyzed to measure their responses using the above assays. The Agilent Seahorse XF Cell Mito Stress Test (six replicates per concentration) was performed to explore mitochondrial function and metabolic pathways. Also, flow cytometry (three replicates per concentration) and laser confocal microscopy (one replicate per concentration) were implemented to study

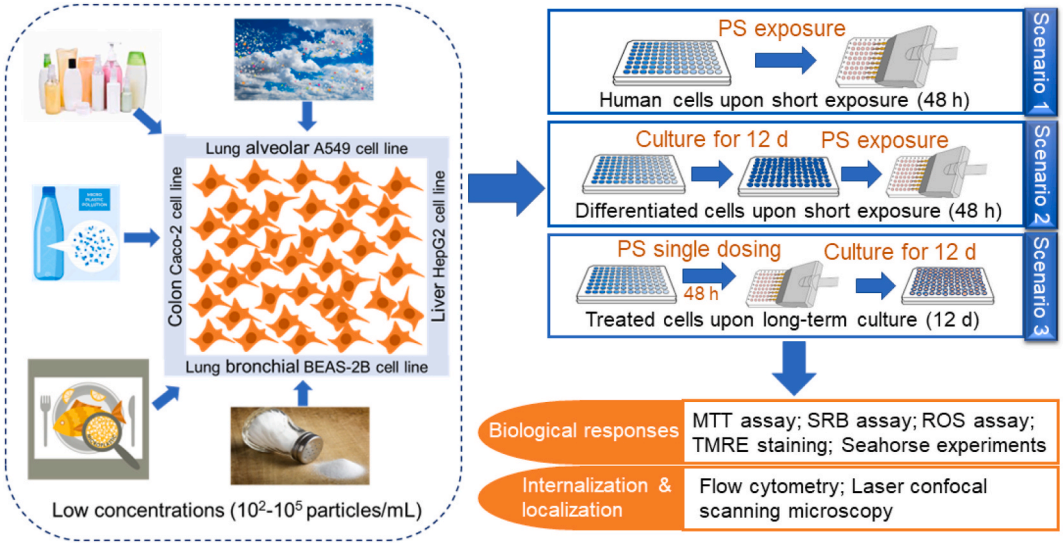

Fig. 1. The schematic overview of the experimental design implemented in this study. Four different cell types were used in the experiment representing the major exposure pathways (inhalation, ingestions, detoxification). The cells were exposed to polystyrene (PS) microparticles in three scenarios with different differentiation status and culture time. After exposure, biological responses and internalization of the PS particles were analyzed.

cellular uptake and localization of PS in cells. For all experiments, culture medium was used as a negative control, and culture medium was changed every 48 h during differentiation.

2.4. Cellular and biochemical assays

Followed by PS exposure, four cellular assays were performed on the above three exposure scenarios to assess cellular and biochemical effects. Before conducting cellular assays, the procedure to exclude possible signals from fluorescent PS was described in supporting information (see Fig. S3 and Fig. S4).

2.4.1. 3-(4,5-dimethylthiazol-2-yl)-2,5-diphenyltetrazolium bromide (MTT) assay

First, six replicates of cells were treated with 10% DMSO for 48 h as positive control. Then 100 μL cell culture medium was removed from each well. Next, 20 μL MTT (final concentration of 5 mg/mL) was added to each well. The treated cells were incubated in the dark for 2 h at 37 °C. After that, all media were carefully removed and 200 μL pure DMSO was added to each well. DMSO solvent was suspended several times to form homogeneous purple solution. Finally, the absorbance of each well was measured at 570 nm with a Spectramax Gemini XS Fluorescence Plate Reader.

2.4.2. Intracellular reactive oxygen species (ROS) assay

First, six replicates of cells were treated with 10% DMSO for 48 h as positive control. Then 20 μM H_2-DCFDA (2,7-dichlorodihydrofluoresceindiacetate) (in 200 μL DMEM without phenol red) was added to each well after removing the old medium. The treated cells were stored in the dark for 20 min at 37 °C. After that, all media were removed and 200 μL phenol red-free DMEM was loaded in each well. Finally, the fluorescence of stained cells was measured by a Spectramax Gemini XS Fluorescence Plate Reader with the excitation and emission wavelengths of 485 and 535 nm, respectively.

2.4.3. Mitochondrial membrane potential assay

First, 1 μM TMRE (tetramethylrhodamine ethyl ester perchlorate) (in 200 μL DMEM without phenol red) was added to each well after removing the old medium. The treated cells were stored in the dark for 30 min at 37 °C. Then cells were washed by 0.2% bovine serum albumin (BSA) in DPBS. After that, 200 μL 0.2% BSA was loaded in each well and the fluorescence of stained cells was measured by a Spectramax Gemini XS Fluorescence Plate Reader with the excitation and emission wavelengths of 549 and 575 nm, respectively. Six replicate wells were exposed to 20 μM FCCP (carbonyl cyanide 4-(trifluoromethoxy) phenylhydrazone) for 10 min at 37 °C as the positive control before TMRE staining.

2.4.4. Sulforhodamine B (SRB) assay

After ROS assay, SRB assay was performed on the same cells that were used for measuring ROS production. First cells in each well were fixed with 50 μL 50% TCA (trichloroacetate) at 4 °C for 1 h. Then the plate was mildly rinsed with tap water five times and was air dried. After that, the cells were stained with SRB solution (0.4% in 1% glacial acetic acid) at room temperature for 30 min. The stained cells were softly rinsed with 1% glacial acetic acid three times and were air dried. Then each well was added 200 μL of 10 mM Tris buffer (Tris(hydroxymethyl)-aminomethane) and was suspended multiple times to form uniform solution. Air bubbles were avoided. Finally, the absorbance of solution was measured at 490 nm by a Spectramax Gemini XS Fluorescence Plate Reader.

2.5. Seahorse analysis of mitochondrial respiration

Human cell lines were seeded in Seahorse 96-well XF Cell Culture microplates (Agilent Seahorse Bioscience, Sana Clara, CA, USA) with 80 μL of culture medium at a density of 8000 cells/well. Cell culture and PS exposure were the same as what was conducted in normal 96-well plates. One day before conducting the XF assay, the Seahorse XF Sensor Cartridge was hydrated by filling 180 μL/well of Seahorse XF Calibrant Solution Cells. Then the prepared cartridge was incubated at 37 °C without CO_2 for 24 h to exclude the interference of CO_2 in the medium to measurements. Before extracellular flux measurements, cells were washed twice with XF Assay Medium (Agilent Seahorse Bioscience, Sana Clara, CA, USA) supplemented with 2 mM glutamine, 1 mM pyruvate and 10 mM glucose and then kept in an incubator at 37 °C without CO_2 for 45 min. After that, the Agilent Seahorse Cell Mito Stress Test was applied to treat cells with a sequential injection of oligomycin (OM) (1 μM and 2 μM for undifferentiated and differentiated cells, respectively), Carbonyl cyanide-4-(trifluoromethoxy) phenylhydrazone (FCCP) (1 μM for undifferntiated A549 and BEAS-2B, 0.5 μM for undifferentiated Caco-2, 0.25 μM for undifferentiated HepG2, 2 μM for differentiated cells), and a mixture of rotenone and antimycin A (ROT/AA) (0.5 μM). Finally, oxygen consumption rate (OCR) and extracellular acidification rate (ECAR) were measured by Agilent Seahorse XFe96 Analyzer (Agilent Seahorse Bioscience, Sana Clara, CA, USA) according to the manufacturer's instructions.

2.6. Microplastics (PS) intake by flow cytometry

After PS exposure, cells were detached with 0.5% Trypsin-EDTA and diluted with PBS. The cell suspension was transferred to a 96-well plate (200 μL per well) for measurement without any staining, and PBS was used as the negative control. The fluorescence emission of PS particles was measured using an Attune NxT flow cytometer equipped with a blue laser (488 nm) and a red laser (637 nm). The number of total cells and cells containing fluorescent PS was counted by gating strategy based on forward scatter, sideward scatter and green fluorescence in the blue laser channel.

2.7. Microplastics (PS) localization by laser confocal microscopy

After PS exposure, cells were washed with PBS. The washed cells were fixed with 4% paraformaldehyde for 20 min at room temperature, followed by washing with PBS. After that, cells were treated with Hoechst 33342 (1000 times of dilution in PBS) for 15 min at room temperature to stain the nuclei. To remove the residual staining, the cells were washed again with PBS. Next, cells were treated with CellMask™ Deep Red plasma (2000 times of dilution in PBS) for 30 min at room temperature to stain the cell membrane. The stained cells were washed with PBS three times. Finally fluorescent images of each stained sample were performed by Nikon A1R confocal microscope from the Centre for Advanced Light Microscopy at Ghent University (Belgium). Images were analyzed with Fiji software 2.1.0.

2.8. Statistical analysis

All the data were normalized based on the negative control (=100%). Statistical analysis was performed using one-way analysis of variance (ANOVA) or non-parametric Kruskal-Wallis test with Tukey post hoc test by R-studio. Statistical significance was indicated as *$p \leq 0.05$. The effect of the positive control was used as quality assurance of the performed assays.

3. Results

Overall, we observed no major effects on cell viability in all treatments (Table1). Most of the effects were related to ROS production while Caco-2 cells showed the most effects under scenario 3 (Table 1). In the next sections, these results will be reported in detail.

Table 1
The overview of cellular and bioenergetic effects of polystyrene microplastic on human cell lines.

	Cell types	MTT assay	SRB assay	TMRE assay	ROS assay	Mitochondrial respiration
Scenario 1	undiff. A549	0	0	0	0	0
	undiff. BEAS-2B	0	↓	0	0	0
	undiff. Caco-2	0	0	0	0	0
	undiff. HepG2	0	0	0	ROS ↑	0
Scenario 2	diff. A549	0	0	0	ROS ↑	0
	diff. Caco-2	0	0	0	0	0
Scenario 3	A549/ long-term culture	0	0	0	ROS ↑	0
	Caco-2/ long-term culture	0	0	MMP	ROS ↑	OCR ↑

(Note: MMP, ROS and OCR refer to mitochondrial membrane potential, reactive oxygen species and oxygen consumption rate, respectively. MTT, SRB, TMRE are abbreviations of chemicals: 3-(4,5-dimethylthiazol-2-yl)-2,5-diphenyltetrazolium bromide, Sulforhodamine B and tetramethylrhodamine ethyl ester perchlorate, resprctively. The arrows represent significant increase or decrease induced by at least one PS concentration. Undifferentiated and differentiated cells are named as undiff. cell (undiff. A549) and diff. cell (diff. A549), respectively.).

3.1. Short-term effects of undifferentiated cells with single PS dosing

3.1.1. Exposure of alveolar and bronchial lung cells

Undifferentiated (confluent) alveolar A549 cells (undiff. A549) were exposed to different concentrations of PS for 48 h as short exposure model. Both mitochondrial activity (MTT assay, Fig. S9A) and protein contents (SRB assay, Fig. S9B) showed the cell viability was not significantly affected by PS at any tested concentration. PS particles did not cause significant effects on mitochondrial membrane potential (Fig. S9C) and ROS production (Fig. S9D) compared to untreated cells. However, ROS production displayed a concentration-dependent trend, ROS value at the highest PS concentration was 23% ($p = 0.009$) higher than that of PS at the lowest concentration. Meanwhile, the parameters of electron transfer chain (ETC) of mitochondrial respiration were measured by serially injected oligomycin (to inhibit ATP synthase, complex V), FCCP (to uncouple oxygen consumption) and mixture of rotenone and antimycin A (to inhibit complexes I and III) (Fig. 2A and C). As shown in Fig. 2B, key mitochondrial parameters, including basal respiration, maximum respiration, proton leak, ATP production, spare respiratory capacity and non-mitochondrial respiration, were not significantly impacted at any concentration of PS. As for undifferentiated bronchial BEAS-2B cells (undiff. BEAS-2B), as displayed in Fig. S10, none of the tested PS concentrations caused significant effects on the mitochondrial activity, mitochondrial membrane potential, ROS production. However, cell viability was significantly inhibited according to the results of SRB assay (Fig. S10B), which decreased to 85% at the highest concentration ($p = 0.028$). The mitochondrial parameters of undiff. BEAS-2B were not affected by any PS dose (Fig. S17).

3.1.2. Exposure of intestinal and hepatic cells

As displayed in Fig. S11 and Fig. S18, undifferentiated intestinal Caco-2 cells (undiff. Caco-2) did not show significant responses on cell viability, mitochondrial membrane potential, ROS generation and mitochondrial functions at any PS dose. Undifferentiated hepatic HepG2 cells (undiff. HepG2) exhibited similar responses to Caco-2 cells with no significant effects on cell viability, mitochondrial membrane potential and mitochondrial respiration (Figs. S12 and S19), while the ROS production at high concentrations was slightly increased compared to untreated cells (Fig. S12D, $p < 0.05$).

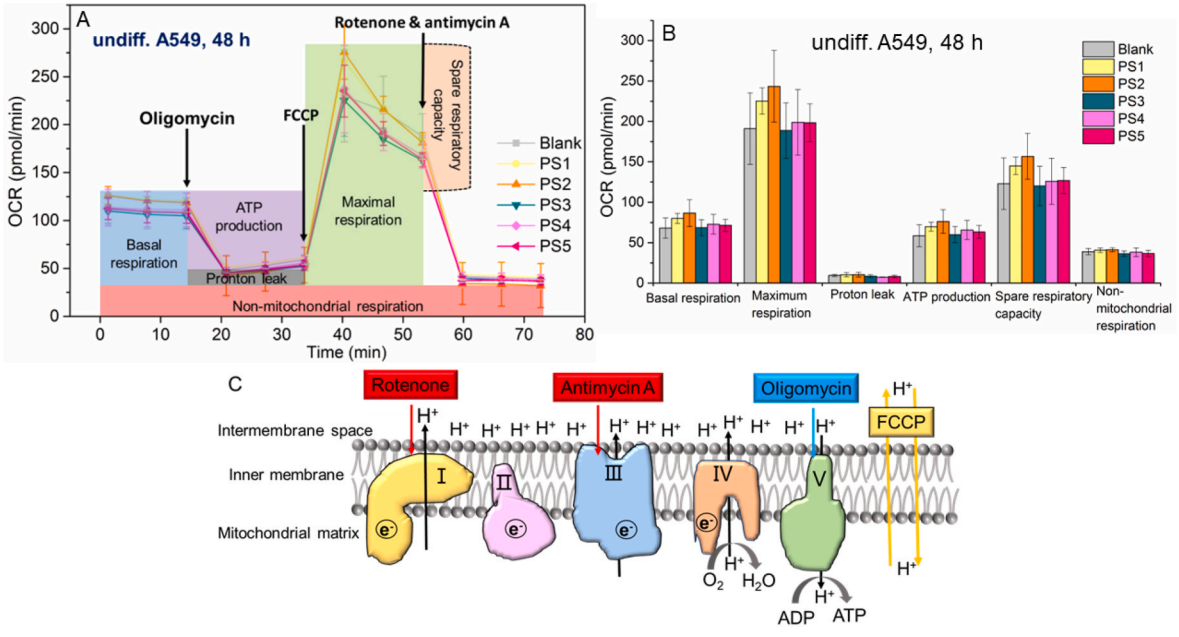

Fig. 2. Effects of PS on mitochondrial respiration of undifferentiated A549 (undiff. A549) cells after 48-h exposure. (A) Mitochondrial profiles of PS-treated undiff. A549 in response to sequential administration of pharmacological modulators of mitochondrial electron transport. (B) Mitochondrial parameters of undiff. A549 cells by measuring oxygen consumption rate (OCR). (C) The electron transfer chain (ETC) in mitochondrial respiration.. (PS1-PS5 correspond to PS concentrations of 1.14×10^2, 1.14×10^3, 1.14×10^4, 5.68×10^4, 5.68×10^5 P/mL, respectively.)

3.2. Short-term effects of differentiated lung and intestinal cells with single PS dosing

Differentiated cells are another vital model for toxicity test which could reflect more physiologically relevant conditions. As explained in the methods section, due to the different abilities of the cell lines to differentiate and maintain differentiation in 2D culture system, this work was specifically conducted with A549 and Caco-2 cells for a period of 14 days.

As scenario 2 depicted in Fig. 1, differentiated A549 and Caco-2 cell lines were exposed to different doses of PS for 48 h to study effects on differentiated cells with short culture. As shown in Fig. S13, cell viability and mitochondrial membrane potential of differentiated A549 cells (diff. A549) were not significantly affected by any PS concentration when compared to negative control. Exposure to PS from 1.14×10^3 to 5.68×10^5 P/mL significantly elevated ROS generation (Fig. S13D), and the ROS value obtained from the second highest dose was about 1.5 times higher than that of negative control ($p = 0.019$). However, the mitochondrial respiration of diff. A549 cells was not affected by any tested PS concentration (Fig. S20). As for differentiated Caco-2 cells (diff. Caco-2) with short exposure, mitochondrial membrane potential, cell viability and ROS production were not significantly changed at any PS concentration when compared to negative control (Fig. S14). Similarly, the mitochondrial respiration of diff. Caco-2 cells was not affected by any tested PS concentration (Fig. S21).

3.3. Long-term effects of lung and intestinal with single PS dosing during differentiation

As scenario 3 depicted in Fig. 1, A549 and Caco-2 cell lines were exposed to PS with single dosing at the beginning of differentiation process to study long-term effects of post-exposure. As illustrated in Fig. S15, mitochondrial membrane potential and cell viability of A549 cells were not altered at any PS concentration. According to ROS assay (Fig. S15D), exposure to PS from 1.14×10^3 to 5.68×10^5 P/mL significantly increased ROS production, and the highest ROS value (measured at 5.68×10^4 P/mL of PS, $p = 0.008$) was about 1.5 times higher than that of the negative control. According to Fig. S22, PS did not lead to significant effects on the mitochondrial respiration after a single dosing exposure of A549 with long-term culture.

As depicted in Fig. S16, Caco-2 cells did not show significant long-term responses on cell viability after exposure during differentiation, while the ROS production and mitochondrial membrane potential were significantly higher than negative control at all tested PS doses (Fig. 3A and B, $p < 0.05$). Moreover, the mitochondrial respiration was affected by PS exposure as well (Fig. 4). Basal respiration (Fig. 4B) and ATP production (Fig. 4C) showed a significant increase when Caco-2 cells were exposed to the three highest concentrations. The proton leak (Fig. 4D) and maximal respiration (Fig. 4E) and were significantly increased at any tested PS dose except the lowest one. All of tested PS concentrations significantly raised spare respiratory capacity compared to the negative control (Fig. 4F).

3.4. Cellular uptake and PS localization

To study the internalization of PS in human cell lines, flow cytometry was used to measure the cellular uptake of PS in four human cell lines. As depicted in Fig. 5A, the fluorescent signals of undifferentiated cells with short culture showed a concentration-dependent trend, which indicated the uptake of fluorescent PS in cells. The uptake rate was different in different cell lines, varying from 18% to 40% at the highest concentration. Generally, undiff. Caco-2 and undiff. BEAS-2B cells showed higher uptake rates compared to undiff. HepG2 and undiff. A549 cells. However, for differentiated cell with short exposure (Fig. 5B), the uptake rate was much lower than that of undifferentiated cells, varying from 1.25% to 2% at the highest dose. Also, the uptake difference between diff. A549 and diff. Caco-2 was smaller than that of two corresponding undifferentiated cell lines, and even diff. A549 cells exhibited slightly higher uptake rate compared to diff. Caco-2 cells. Moreover, the uptake rates in scenario 3 were studied as well. A549 and Caco-2 cells were exposed to single PS dosing (5.68×10^5 P/mL) with 14-d post-exposure. Fluorescent signals were recorded by flow cytometry every 48 h. As displayed in Fig. 5C, in accordance with the uptake order of undifferentiated cells, the uptake rate of Caco-2 cells was significantly higher than that of A549 cells during their differentiation. Furthermore, the uptake rate at 2 days was set 100%, and the following uptake values were normalized by it to see internalization and release of PS during differentiation. Specifically, the uptake rates of both cells in this exposure scenario showed moderate fluctuation during the increment of exposure time but with a decreasing trend on the whole. The relative uptake rate after 14 days declined to 62.99% and 66.51% for A549 and Caco-2, respectively (Fig. 5D).

Based on measurements from flow cytometry, PS particles seem to be able to enter four human cell lines, albeit in different degrees. The localization of fluorescent PS in cell lines was analyzed by confocal microscopy. However, the high fluorescent intensity of PS combined with a limited resolution in the z-axis (resulting in point spread function) complicated the interpretation of the images. As illustrated in Fig. S23, PS particles seem to be internalized in undifferentiated cells upon short exposure and indications of transfer of PS into nuclei could be observed as well. In addition, PS particles could be internalized in cell membrane and nuclei of differentiated A549 and Caco-2 cells with short exposure as well (Fig. 6A and B and Fig. S24). The same phenomena of PS localization could be observed when A549 and Caco-2 cells were exposed to single PS dosing after 12-d culture (Fig. 6C and D and Fig. S25).

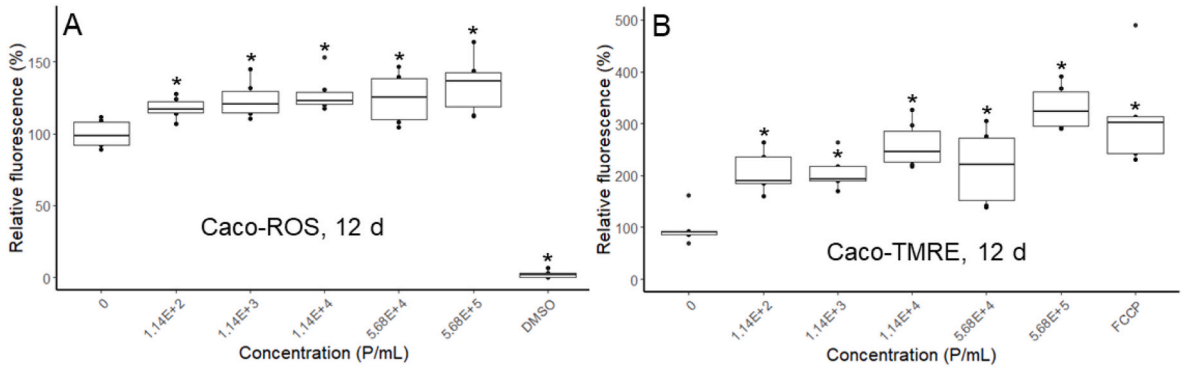

Fig. 3. (A) Relative ROS production and (B) mitochondrial membrane potential of Caco-2 cells exposed to different concentrations of PS with 12-d culture; DMSO and FCCP are the positive control of ROS and SRB assays, respectively; $n = 6$; *$p \leq 0.05$, significant difference from negative control.

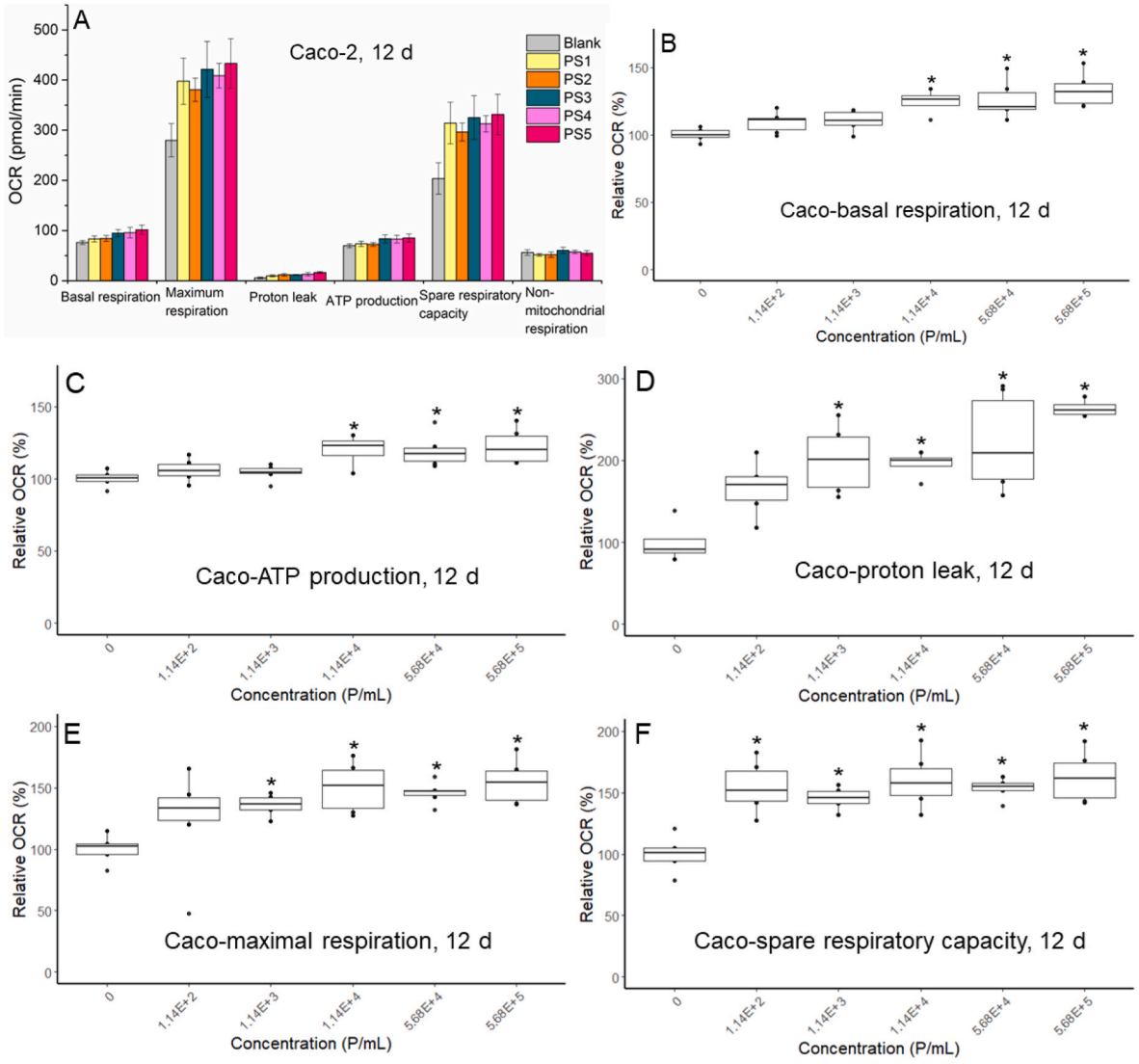

Fig. 4. Effects of PS on mitochondrial respiration of Caco-2 cells with 12-d culture. (A) Mitochondrial parameters in Caco-2 cells by measurement of oxygen consumption rate (OCR) (A). Relative OCR from basal respiration (B), ATP production (C), proton leak (D) and maximal respiration (E) and spare respiratory capacity (F) in Caco-2 cells. n = 6; *p ≤ 0.05, significant difference from negative control.. (PS1-PS5 correspond to PS concentrations of 1.14×10^2, 1.14×10^3, 1.14×10^4, 5.68×10^4, 5.68×10^5 P/mL, respectively.)

4. Discussion

Microplastics (MPs) are ubiquitous in our living environment, which raises concerns regarding daily exposure and cause potentially negative effects on human health. Up to date, there are plenty of studies detecting microplastics in drinking water, fruits, vegetables and aquatic food. For insoluble plastic particles, it is supposed that particles number concentration (particles/mL) would be more informative than mass concentration or other units when it comes to interaction and effects with cells. However, converting MPs concentration from the above solid sources (see Table S2) into unit of particles/mL could be disputable due to some unfixed parameters. Therefore, we only summarized detected concentrations in liquid and found the highest reported concentration is about 10^4 particles/mL (see Table S2). Moreover, currently it is reported that the mean concentration of plastic particles detected in human blood was 1.6 μg/mL, which equals to 3.64×10^5 particles/mL if 2-μm polystyrene (PS) particles used in this work were implemented in the conversion (Leslie et al., 2022). Integrating the above reported concentrations together, we set 10^5 particles/mL as the highest dose for exposure to rationally evaluate effects of MPs on human health. In general, plastic particles could be ingested in the gut and be respirated in the lung. Once plastic particles are internalized by those epithelial lung or gut cells, they could be transported into circulatory systems and possibly enter cells correlated with physiological transport through the liver by the portal vein. To support more realistic effect assessments in the future, four human cell lines (A549, BEAS-2B, Caco-2 and HepG2), representing pathways of inhalation and ingestion as well as potential detoxification, with different differentiation status and culture scenarios were comprehensively assessed in this study.

Four undifferentiated cell lines exposed to single PS dosing with short exposure (48 h, scenario 1) showed no significant effects on cell survival at all tested concentrations. Recent literature has indicated that oxidative stress or overproduction of ROS is one of the key mechanisms by which MPs affect cells since excessive ROS production could lead to the potential damage to macromolecules such as nucleic acids, lipids and proteins (Jeon et al., 2021; Rubio et al., 2020; Wei et al., 2022; Xie et al., 2020). Examples include the expression of stress-response proteins (HO-1 and HSP70) and of proinflammatory cytokines (IL-6 and IL-8) due to high ROS levels (Dong et al., 2020; Wu et al., 2019). In this scenario, we only observed statistically significant high ROS levels in undiff.

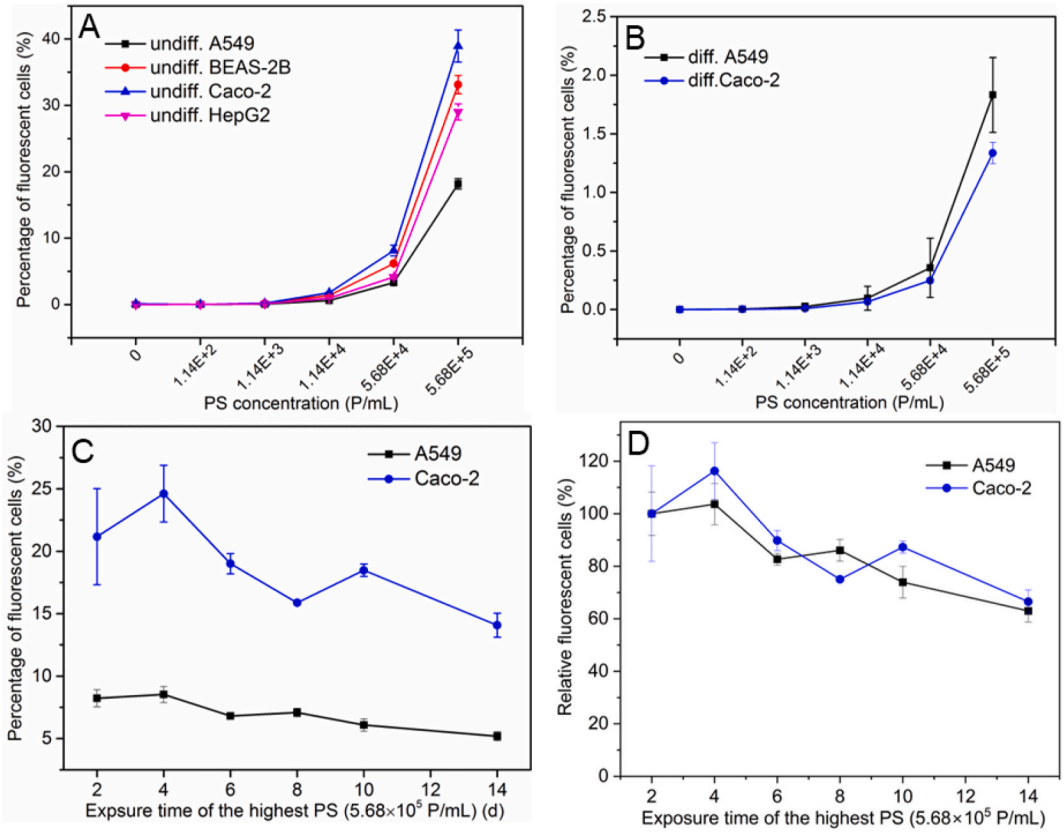

Fig. 5. The percentage of fluorescent cells over the total population in (A) undifferentiated cells and (B) differentiated cells exposed to PS for 48 h and in (C) cell lines exposed to the single PS dosing (5.68×10^5 P/mL) with 14-d post-exposure by flow cytometry; (D) The relative fluorescent cells at different time points based on data from Fig. 5C (The value at 2 days, which is the end of PS exposure as PS suspension was replaced by culture medium at this timeslot, was set as 100%, other values at later timeslots were normalized by data at 2 days); n = 3.

HepG2 cells at high PS concentrations. A possible reason for this observation is that HepG2 cells need to generate more ROS to overcome the stress to achieve self-resistance (Chen et al., 2022). The mitochondria are the key organelles that represent the bioenergetic status of cells where mitochondrial respiration is the main activity that consumes oxygen to sustain oxidative metabolism (Piquereau et al., 2013; Ye et al., 2011). In order to investigate possible effects of PS on aerobic energy pathway (oxidative phosphorylation), we used the Agilent Seahorse XFe96 Analyzer to measure key mitochondrial parameters of four undifferentiated cell lines. Mitochondrial functions of four undifferentiated cell lines did not exhibit significant response at any PS concentration, indicating that they are tolerant to stress from PS exposure. As such, the increased ROS in undiff. HepG2 was likely from other sources such as glycolysis, enzymatic reactions, cytokines and growth promoters that were reported in fish treated with PS particles (Umamaheswari et al., 2021), instead of from mitochondria which are regarded as the main source of ROS in living cells (Feissner et al., 2009). Specifically, the electron transfer chain (ETC) complex I and III are the major mitochondrial sites that produce ROS (superoxide, $O_2^{\cdot-}$) by univalent reduction of O_2 (Brand et al., 2004; Kussmaul and Hirst, 2006). Overall, at a cellular level, PS at relatively low concentrations is unlikely to result in negative effects on undifferentiated cells under short exposure even if PS particles were internalized in cells, which is different from most of the published results that demonstrated significant cytotoxicity and ROS production in A549, BEAS-2B and Caco-2 cells (Cortés et al., 2020; Dong et al., 2020; Goodman et al., 2021; Wu et al., 2019; Xu et al., 2019). The lack of response here can primarily be attributed to the lower concentrations used in our study compared to the published research (see Table S1). From the perspective of mitochondria, to the best of our knowledge, only a few papers reported significant responses on spare respiratory capacity, proton leak and ATP production when A549, L-02 and BEAS-2B cells were exposed to high nanoplastics concentrations (Halimu et al., 2022; Lin et al., 2022; Wang et al., 2022). Our work is the first study to investigate impacts of microplastics on the mitochondrial functions in different cell types under multiple exposure scenarios, which clearly shows micro-PS at currently reported human exposure levels did not impair mitochondrial functions after short exposure.

The same assays were performed on differentiated A549 and Caco-2 cell lines with short exposure to support more relevant effect assessments. Only one endpoint, ROS production, was significantly elevated in diff. A549 cells exposed to high PS, which is in line with a study that reported A549 cells consumed more oxygen and produced higher ROS levels during differentiation (Ye et al., 2011). Similarly, the differentiated neuronal cells exhibited significant ROS production and tended to suffer oxidant mediated-damage because of the different activities of essential antioxidant enzymes and a limited ability to produce or recycle glutathione during differentiation (Sivanantham et al., 2018). However, diff. Caco-2 cells did not show any significant cellular and mitochondrial response, which was the same as what was observed in undiff. Caco-2 cells. Further molecular parameters could help to elucidate the different modes of action for Caco-2 cells with different differentiation states in future studies.

Different from most chronic studies with continuous contaminants exposure conducted to date (Domenech et al., 2021; Visalli et al., 2021; Xi et al., 2019), a novel strategy used in this study was to expose A549 and Caco-2 cells to PS once and follow the biological responses by 12-d post-exposure to explore long-term effects after a single dosing (scenario 3). A key focus here was to assess the potential long-term effects of residual particles in and outside the cells after the initial exposure. Compared to the above two scenarios with short exposure, A549 and

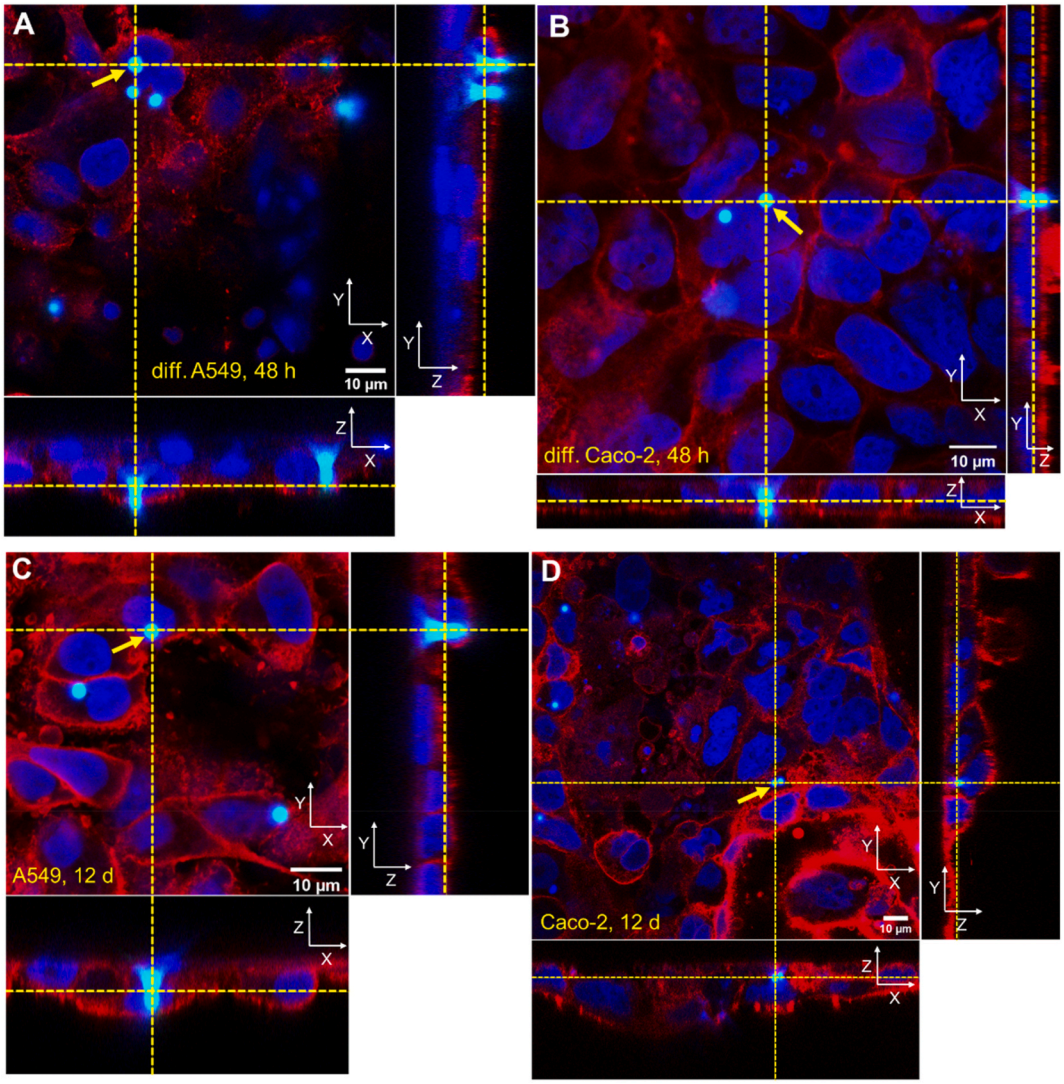

Fig. 6. Three-dimensional images of human cell lines taken by confocal microscopy after exposure to the highest PS (5.68×10^5 P/mL). (A) Differentiated A549 and (B) Caco-2 cells were exposed to PS for 48 h; (C) A549 and (D) Caco-2 cells were exposed to single PS dosing after 12-d culture during differentiation process. Nuclei and cell membranes were stained to show blue and red fluorescence, respectively. PS exhibited green and blue fluorescence. Yellow lines point out the plane from where the orthogonal views are projected. The left, bottom and right mages were viewed from XY, XZ and YZ panels, respectively.

Caco-2 cells with long-term culture during differentiation, exhibited significant stimulation on ROS production and mitochondrial membrane potential from low to high concentrations of PS. It demonstrates that reaction mechanism of both cells on PS with long-term culture is quite different from the responses of cells with short culture. There are the following possible explanations: 1) followed by single PS dosing, long-term culture caused persistent and accumulated oxidative stress on cells and even probably damaged the integrity of mitochondria of Caco-2; 2) both cells with the altered phenotype and cell morphology during differentiation were likely to be more sensitive to PS; 3) PS probably induced more toxic effects on cell differentiation than proliferation. Unfortunately, no related or similar studies could support or correspond to our hypothesis.

It is worthwhile to highlight that mitochondrial respiration of Caco-2 cells with long-term culture was affected by PS treatment as well. Specifically, five mitochondrial respiration parameters were significantly increased from low to high PS concentrations. This demonstrates single PS dosing with long-term culture stimulated Caco-2 cells to improve energetic demand to cope with the stress from PS. The possible explanations to these phenomena are in the following: 1) the electron transfer chain (ETC, see Fig. 2C) in mitochondria, suffering persistent and accumulated oxidative stress from PS exposure, would consume more oxygen and produce more ATP to reach self-resistance; 2) the observed high membrane potential (Fig. 3B) indicates that PS impaired mitochondrial functions and disrupted the balance of H^+ transfer between mitochondrial matrix and inner membrane, leading to larger synthesis of ATP at higher potential that is stated by the literature (Zorova et al., 2018); 3) the significant increase in proton leak is probably attributed to the damage to ETC complexes or the inner membrane, suggesting mitochondrial injury. It is reported that ETC could generate significantly increased ROS at high mitochondrial membrane potential (Skulachev, 1996; Starkov and Fiskum, 2003), which might be one of reasons that ROS production increased upon PS exposure in our study. It is worthwhile to mention that non-mitochondrial respiration, oxygen consumption persisting due to a subset of cellular enzymes that continue to consume oxygen, did not change at any PS dose. It suggests our results are an accurate measure of mitochondrial respiration based on the same level of oxygen consumption rate (OCR). Based on the above results, it is clear that single PS dosing caused more oxidative stress on A549 and Caco-2 cells with long-term culture and evoked mitochondrial dysfunction of Caco-2 compared to short culture. However, the effects caused by such stress are not acutely detrimental for cells, and it only

influenced mitochondrial respiration chain. One possible reason is that the concentration we used is quite low, which may be below the threshold of lethal dose. Another explanation is that cells have complicated mechanisms able to regulate mitochondrial quantity, quality and homeostasis. Some research demonstrated that mitochondrial homeostasis is achieved through synergetic processes such as mitochondrial biogenesis, and thus, some mitochondrial parameters (such as spare respiratory capacity levels and ATP transfer) are regulated by these mitochondrial quality control mechanisms (Marchetti et al., 2020).

Overall, we primarily observed elevated effects on ROS production and mitochondrial respiration. A recent adverse outcome pathway developed by Jeong indicated that ROS production could induce oxidative stress and inflammation response and eventually lead to potential higher level effects including growth reduction, reproductive failure and even mortality (Jeong and Choi, 2019). Moreover, mitochondrial dysfunction under oxidative stress implies potential pathogenesis of multiple human metabolic disorders (diabetes, obesity), cancer, cardiovascular disease and neurodegeneration (Camara et al., 2011; Camara et al., 2009; Cortassa et al., 2014; Wang et al., 2023). Our results further highlight the role of ROS and mitochondrial functions as the molecular and metabolic initiating events to assess micro-PS ecotoxicity. Further studies should confirm the downstream reaction into other tissues and organs. Also, the above observable end-points did not show a clear concentration dependence response, which could be attributed that our concentration range particularly focused on the lower part of the concentration response curve in terms of particle number. It could reflect more realistic exposure levels in human daily life.

The internalization and localization of fluorescent particles revealed that PS could be internalized in cell membrane and nuclei during short exposure as depicted in confocal images. This phenomenon was consistent with previous studies that detected PS particles in undifferentiated A549, HepG2 and Caco-2 cell lines (Cortés et al., 2020; Goodman et al., 2021; He et al., 2020). Also, due to that the gentle PBS wash used in this work to avoid damage to cells is probably not able to break the binding force between PS particles and cell membrane, some particles absorbed on the surface of cells were observed as well (such as Fig. S23G). However, not only the internalized microplastics, but also absorbed particles would induce biological effects on cells, which was reported by another literature as well (Goodman et al., 2021). Thus, absorbed microplastics are another vital contributor to biological effects and could not be ignored. In contrast to high uptake rates in undifferentiated cells, differentiated A549 and Caco-2 cells exhibited lower uptake rate of PS. There are two possible reasons for these results: 1) the number of differentiated cells are much higher than undifferentiated cells (about three times) as the culture time of differentiated cells is much longer than that of undifferentiated cells (Gerloff et al., 2013); 2) the altered phenotype and cell morphology after differentiation are likely to diminish the capability of the uptake of microplastics in differentiated cells. Previous research also observed that undifferentiated Caco-2 cells had much higher ability to internalize graphene oxide sheets than differentiated cells (Kucki et al., 2017). The lower uptake rate is probably one of the reasons of absence of significant effects in differentiated cells as biological effects are expected to be correlated to high internalized plastic particle number in cells (da Silva Brito et al., 2023).

Similar to cells with short exposure, PS particles were observed in cell membrane and even in nuclei of scenario 3 where A549 and Caco-2 cells were exposed to single PS dosing with 12-d post-exposure. It is interesting to highlight the dynamic uptake and release once cells were exposed to PS at the beginning of differentiation process. As in line with the results of undifferentiated cells, the uptake rate of Caco-2 cells was rather higher than that of A549 cells during differentiation, which may be a reason that PS induced more stimulated long-term effects on Caco-2 cells than that on A549 cells. A study also reported that induction of defensive responses (significant oxidative and mitochondrial stress) related to high number of plastic particles in Caco-2 cells (Saenen et al., 2023). The internalization of PS in both cells fluctuated with the increment of exposure time and the final relative uptake rates remained more than 60%. The possible explanation is that PS could be accumulated in cells by pinocytosis/micropinocytosis or by phagocytosis without any specific receptor, and the internalization saturation occurred within certain time followed by release process (Xu et al., 2019). In addition, cells would grow and die during differentiation, and thus PS will be released and internalized repeatedly. More importantly, it is very difficult for cells to excrete micro-PS particles once they are internalized in cells, which corresponds to the above results that long-term culture showed more negative effects than short culture. In other words, due to the retention of PS in cells, potential harmful effects would appear in our body with single intake after a long time. As stated in the above, the continuous metabolic and oxidative stress are on the onset of many chronic diseases. Whether this is occurring as a result of PS exposure remains to be elucidated.

These results thus show for the first time that single intake of micro-PS in the human body is not likely to cause detrimental effects for short period but might trigger stress after a long time. Evidently, to be able to estimate the impact of microplastics on human health, in the full continuum of plastic types, sizes and shapes, similar experiments would be necessary by using more variable plastic particles. Moreover, the effects of additives, surface coatings and weathering, amongst others, should be tested to be able to estimate the relevant risk of plastic exposure for human health. Moreover, apart from carcinogenic cell lines, normal cell lines (such as L-02 and NCM460) would be appropriate cell models to study in vitro toxicological effects too as they are more relevant for transcriptomic studies given the gene expression differences between normal and carcinogenic cell lines.

5. Conclusions

In this study, A549, BEAS-2B, Caco-2 and HepG2 cell lines were exposed to 2-μm PS at tested concentrations close to currently reported human exposure levels (no more than 10^5 particles/mL) under three mimicked scenarios. PS could be internalized in cell membrane and even in the nuclei for all tested cell lines but undifferentiated Caco-2 cells showed the highest uptake rate without any cell survival loss and mitochondrial dysfunction after short exposure. No statistically significant changes in cell viability and mitochondrial functions were observed in both undifferentiated and differentiated cell lines with short exposure even if undifferentiated cells showed higher uptake rates. It is worthwhile to note that the exposure of single PS dosing followed by long-term culture resulted in negative effects on Caco-2 cells, which showed overproduction of ROS, higher mitochondrial membrane potential and stimulated mitochondrial respiration. It suggests that single PS dosing could disrupt electron transfer chain to evoke mitochondrial damage and break the balance of H^+ transport between the mitochondrial matrix and mitochondrial inner membrane during 12-d differentiation process. Similarly, A549 cells with long-term culture were more sensitive to oxidative stress of PS than A549 cells upon short culture. This work investigates the impacts of PS microplastic on cell type, cell differentiation status and post-exposure time at low concentrations.

Declaration of competing interest

The authors declare that they have no known competing financial interests or personal relationships that could have appeared to influence the work reported in this paper.

Data availability

Data will be made available on request.

Acknowledgements

Miao Peng is funded by China Scholarship Council (CSC) (File No. 201906150135) and UGent special research fund (BOFCHN2019000801) during her PhD study. Maaike Vercauteren is supported by the BOF-research grant (grant code BOF21/PDO/081). We thank the Special Research Fund from Ghent University for funding the Seahorse equipment (BOF.BAS.2020.0035.01). This research work was partially funded by the project ImpTox, an European Union's Horizon 2020 research and innovation program under the grant No 965173. We greatly appreciate the help of João Alves Barbosa with the cell culture and Herlinde De Keersmaecker for her help on parameters setting of confocal microscopy. We thank the Centre for Advanced Light Microscopy at Ghent University (Belgium) for the use and support on confocal microscopy as well.

Appendix A. Supplementary data

Supplementary data to this article can be found online at https://doi.org/10.1016/j.envpol.2023.122550.

References

Alimi, O.S., Farner Budarz, J., Hernandez, L.M., Tufenkji, N., 2018. Microplastics and nanoplastics in aquatic environments: aggregation, deposition, and enhanced contaminant transport. Environ. Sci. Technol. 52 (4), 1704–1724.
Amato-Lourenço, L.F., Carvalho-Oliveira, R., Júnior, G.R., dos Santos Galvão, L., Ando, R.A., Mauad, T., 2021. Presence of airborne microplastics in human lung tissue. J. Hazard Mater. 416, 126124.
Arzumanian, V.A., Kiseleva, O.I., Poverennaya, E.V., 2021. The Curious Case of the HepG2 Cell Line: 40 Years of Expertise.
Bonanomi, M., Salmistraro, N., Porro, D., Pinsino, A., Colangelo, A.M., Gaglio, D., 2022. Polystyrene micro and nano-particles induce metabolic rewiring in normal human colon cells: a risk factor for human health. Chemosphere 303, 134947.
Braga, A.R.C., Murador, D.C., de Souza Mesquita, L.M., de Rosso, V.V., 2018. Bioavailability of anthocyanins: gaps in knowledge, challenges and future research. J. Food Compos. Anal. 68, 31–40.
Brand, M.D., Affourtit, C., Esteves, T.C., Green, K., Lambert, A.J., Miwa, S., Pakay, J.L., Parker, N., 2004. Mitochondrial superoxide: production, biological effects, and activation of uncoupling proteins. Free Radical Biol. Med. 37 (6), 755–767.
Bruinink, A., Wang, J., Wick, P., 2015. Effect of particle agglomeration in nanotoxicology. Arch. Toxicol. 89 (5), 659–675.
Camara, A., Bienengraeber, M., Stowe, D., 2011. Mitochondrial approaches to protect against cardiac ischemia and reperfusion injury. Front. Physiol. 2.
Camara, A.K.S., Lesnefsky, E.J., Stowe, D.F., 2009. Potential therapeutic benefits of strategies directed to mitochondria. Antioxid. Redox Signaling 13 (3), 279–347.
Chen, X., Abdallah, M.F., Grootaert, C., Rajkovic, A., 2022. Bioenergetic status of the intestinal and hepatic cells after short term exposure to fumonisin B1 and aflatoxin B1. Int. J. Mol. Sci. 23 (13), 6945.
Connors, K.A., Dyer, S.D., Belanger, S.E., 2017. Advancing the quality of environmental microplastic research. Environ. Toxicol. Chem. 36 (7), 1697–1703.
Cooper, J.R., Abdullatif, M.B., Burnett, E.C., Kempsell, K.E., Conforti, F., Tolley, H., Collins, J.E., Davies, D.E., 2016. Long term culture of the A549 cancer cell line promotes multilamellar body formation and differentiation towards an alveolar type II pneumocyte phenotype. PLoS One 11 (10), e0164438.
Corbière, V., Dirix, V., Norrenberg, S., Cappello, M., Remmelink, M., Mascart, F., 2011. Phenotypic characteristics of human type II alveolar epithelial cells suitable for antigen presentation to T lymphocytes. Respir. Res. 12 (1), 15.
Cortassa, S., O'Rourke, B., Aon, M.A., 2014. Redox-Optimized ROS Balance and the relationship between mitochondrial respiration and ROS. Biochim. Biophys. Acta 1837 (2), 287–295.
Cortés, C., Domenech, J., Salazar, M., Pastor, S., Marcos, R., Hernández, A., 2020. Nanoplastics as a potential environmental health factor: effects of polystyrene nanoparticles on human intestinal epithelial Caco-2 cells. Environ. Sci.: Nano 7 (1), 272–285.
da Silva Brito, W.A., Singer, D., Miebach, L., Saadati, F., Wende, K., Schmidt, A., Bekeschus, S., 2023. Comprehensive in vitro polymer type, concentration, and size correlation analysis to microplastic toxicity and inflammation. Sci. Total Environ. 854, 158731.
Dalla Fontana, G., Mossotti, R., Montarsolo, A., 2020. Assessment of microplastics release from polyester fabrics: the impact of different washing conditions. Environ. Pollut. 264, 113960.
Domenech, J., de Britto, M., Velázquez, A., Pastor, S., Hernández, A., Marcos, R., Cortés, C., 2021. Long-term effects of polystyrene nanoplastics in human intestinal caco-2 cells. Biomolecules 11 (10).
Dong, C.-D., Chen, C.-W., Chen, Y.-C., Chen, H.-H., Lee, J.-S., Lin, C.-H., 2020. Polystyrene microplastic particles: in vitro pulmonary toxicity assessment. J. Hazard Mater. 385, 121575.
Elkhatib, D., Oyanedel-Craver, V., 2020. A critical review of extraction and identification methods of microplastics in wastewater and drinking water. Environ. Sci. Technol. 54 (12), 7037–7049.
Fadare, O.O., Wan, B., Guo, L.-H., Zhao, L., 2020. Microplastics from consumer plastic food containers: are we consuming it? Chemosphere 253, 126787.
Feissner, R.F., Skalska, J., Gaum, W.E., Sheu, S.S., 2009. Crosstalk signaling between mitochondrial Ca2+ and ROS. Front. Biosci. 14 (4), 1197–1218.
Gasperi, J., Wright, S.L., Dris, R., Collard, F., Mandin, C., Guerrouache, M., Langlois, V., Kelly, F.J., Tassin, B., 2018. Microplastics in air: are we breathing it in? Curr. Opin. Environ. Sci. Health 1, 1–5.
Gautam, R., Jo, J., Acharya, M., Maharjan, A., Lee, D., K C, P.B., Kim, C., Kim, K., Kim, H., Heo, Y., 2022. Evaluation of potential toxicity of polyethylene microplastics on human derived cell lines. Sci. Total Environ. 838, 156089.
Geirnaert, A., Calatayud, M., Grootaert, C., Laukens, D., Devriese, S., Smagghe, G., De Vos, M., Boon, N., Van de Wiele, T., 2017. Butyrate-producing bacteria supplemented in vitro to Crohn's disease patient microbiota increased butyrate production and enhanced intestinal epithelial barrier integrity. Sci. Rep. 7 (1), 11450.
Gerloff, K., Pereira, D.I.A., Faria, N., Boots, A.W., Kolling, J., Förster, I., Albrecht, C., Powell, J.J., Schins, R.P.F., 2013. Influence of simulated gastrointestinal conditions on particle-induced cytotoxicity and interleukin-8 regulation in differentiated and undifferentiated Caco-2 cells. Nanotoxicology 7 (4), 353–366.
Goodman, K.E., Hare, J.T., Khamis, Z.I., Hua, T., Sang, Q.-X.A., 2021. Exposure of human lung cells to polystyrene microplastics significantly retards cell proliferation and triggers morphological changes. Chem. Res. Toxicol. 34 (4), 1069–1081.
Halimu, G., Zhang, Q., Liu, L., Zhang, Z., Wang, X., Gu, W., Zhang, B., Dai, Y., Zhang, H., Zhang, C., Xu, M., 2022. Toxic effects of nanoplastics with different sizes and surface charges on epithelial-to-mesenchymal transition in A549 cells and the potential toxicological mechanism. J. Hazard Mater. 430, 128485.
He, Y., Li, J., Chen, J., Miao, X., Li, G., He, Q., Xu, H., Li, H., Wei, Y., 2020. Cytotoxic effects of polystyrene nanoplastics with different surface functionalization on human HepG2 cells. Sci. Total Environ. 723, 138180.
Hernandez, L.M., Yousefi, N., Tufenkji, N., 2017. Are there nanoplastics in your personal care products? Environ. Sci. Technol. Lett. 4 (7), 280–285.
Hidalgo, I.J., Raub, T.J., Borchardt, R.T., 1989. Characterization of the human colon carcinoma cell line (Caco-2) as a model system for intestinal epithelial permeability. Gastroenterology 96 (3), 736–749.
Jeon, S., Lee, D.-K., Jeong, J., Yang, S.I., Kim, J.-S., Kim, J., Cho, W.-S., 2021. The reactive oxygen species as pathogenic factors of fragmented microplastics to macrophages. Environ. Pollut. 281, 117006.
Jeong, J., Choi, J., 2019. Adverse outcome pathways potentially related to hazard identification of microplastics based on toxicity mechanisms. Chemosphere 231, 249–255.
Kucki, M., Diener, L., Bohmer, N., Hirsch, C., Krug, H.F., Palermo, V., Wick, P., 2017. Uptake of label-free graphene oxide by Caco-2 cells is dependent on the cell differentiation status. J. Nanobiotechnol. 15 (1), 46.
Kussmaul, L., Hirst, J., 2006. The mechanism of superoxide production by NADH: ubiquinone oxidoreductase (complex I) from bovine heart mitochondria. Proc. Natl. Acad. Sci. USA 103 (20), 7607–7612.
Kutralam-Muniasamy, G., Pérez-Guevara, F., Elizalde-Martínez, I., Shruti, V.C., 2020. Branded milks – are they immune from microplastics contamination? Sci. Total Environ. 714, 136823.
Leslie, H.A., van, J.M., Velzen, M., Brandsma, S.H., Vethaak, D., Garcia-Vallejo, J.J., Lamoree, M.H., 2022. Discovery and quantification of plastic particle pollution in human blood. Environ. Int., 107199
Lever, J.E., 1979. Regulation of dome formation in differentiated epithelial cell cultures. J. Supramol. Struct. 12 (2), 259–272.
Liebezeit, G., Liebezeit, E., 2013. Non-pollen particulates in honey and sugar. Food Addit. Contam. 30 (12), 2136–2140.
Lin, S., Zhang, H., Wang, C., Su, X.-L., Song, Y., Wu, P., Yang, Z., Wong, M.-H., Cai, Z., Zheng, C., 2022. Metabolomics reveal nanoplastic-induced mitochondrial damage in human liver and lung cells. Environ. Sci. Technol. 56 (17), 12483–12493.
Liu, C.-S., Glahn, R.P., Liu, R.H., 2004. Assessment of carotenoid bioavailability of whole foods using a caco-2 cell culture model coupled with an in vitro digestion. J. Agric. Food Chem. 52 (13), 4330–4337.
Liu, L., Xu, K., Zhang, B., Ye, Y., Zhang, Q., Jiang, W., 2021. Cellular internalization and release of polystyrene microplastics and nanoplastics. Sci. Total Environ. 779, 146523.
Liu, S., Wu, X., Gu, W., Yu, J., Wu, B., 2020. Influence of the digestive process on intestinal toxicity of polystyrene microplastics as determined by in vitro Caco-2 models. Chemosphere 256, 127204.
Marchetti, P., Fovez, Q., Germain, N., Khamari, R., Kluza, J., 2020. Mitochondrial spare respiratory capacity: mechanisms, regulation, and significance in non-transformed and cancer cells. Faseb. J. 34 (10), 13106–13124.
Mohammed, F.A., Elkady, A.I., Syed, F.Q., Mirza, M.B., Hakeem, K.R., Alkarim, S., 2018. Anethum graveolens (dill) – a medicinal herb induces apoptosis and cell cycle arrest in HepG2 cell line. J. Ethnopharmacol. 219, 15–22.
Natoli, M., Leoni, B.D., D'Agnano, I., D'Onofrio, M., Brandi, R., Arisi, I., Zucco, F., Felsani, A., 2011. Cell growing density affects the structural and functional properties of Caco-2 differentiated monolayer. J. Cell. Physiol. 226 (6), 1531–1543.
Persoz, C., Achard, S., Leleu, C., Momas, I., Seta, N., 2010. An in vitro model to evaluate the inflammatory response after gaseous formaldehyde exposure of lung epithelial cells. Toxicol. Lett. 195 (2), 99–105.
Persoz, C., Achard, S., Momas, I., Seta, N., 2012. Inflammatory response modulation of airway epithelial cells exposed to formaldehyde. Toxicol. Lett. 211 (2), 159–163.

Pichardo, S., Devesa, V., Puerto, M., Vélez, D., Cameán, A.M., 2017. Intestinal transport of Cylindrospermopsin using the Caco-2 cell line. Toxicol. Vitro 38, 142–149.
Piquereau, J., Caffin, F., Novotova, M., Lemaire, C., Veksler, V., Garnier, A., Ventura-Clapier, R., Joubert, F., 2013. Mitochondrial dynamics in the adult cardiomyocytes: which roles for a highly specialized cell? Front. Physiol. 4.
Ragusa, A., Svelato, A., Santacroce, C., Catalano, P., Notarstefano, V., Carnevali, O., Papa, F., Rongioletti, M.C.A., Baiocco, F., Draghi, S., D'Amore, E., Rinaldo, D., Matta, M., Giorgini, E., 2021. Plasticenta: first evidence of microplastics in human placenta. Environ. Int. 146, 106274.
Ramaiahgari, S.C., den Braver, M.W., Herpers, B., Terpstra, V., Commandeur, J.N.M., van de Water, B., Price, L.S., 2014. A 3D in vitro model of differentiated HepG2 cell spheroids with improved liver-like properties for repeated dose high-throughput toxicity studies. Arch. Toxicol. 88 (5), 1083–1095.
Rubio, L., Barguilla, I., Domenech, J., Marcos, R., Hernández, A., 2020. Biological effects, including oxidative stress and genotoxic damage, of polystyrene nanoparticles in different human hematopoietic cell lines. J. Hazard Mater. 398, 122900.
Saenen, N.D., Witters, M.S., Hantoro, I., Tejeda, I., Ethirajan, A., Van Belleghem, F., Smeets, K., 2023. Polystyrene microplastics of varying sizes and shapes induce distinct redox and mitochondrial stress responses in a caco-2 monolayer. Antioxidants 12 (3), 739, 2023.
Sana, S.S., Dogiparthi, L.K., Gangadhar, L., Chakravorty, A., Abhishek, N., 2020. Effects of microplastics and nanoplastics on marine environment and human health. Environ. Sci. Pollut. Res. 27 (36), 44743–44756.
Schwabl, P., Köppel, S., Königshofer, P., Bucsics, T., Trauner, M., Reiberger, T., Liebmann, B., 2019. Detection of various microplastics in human stool. Ann. Intern. Med. 171 (7), 453–457.
Sivanantham, B., Krishnan, U., Rajendiran, V., 2018. Amelioration of oxidative stress in differentiated neuronal cells by rutin regulated by a concentration switch. Biomed. Pharmacother. 108, 15–26.
Skulachev, V.P., 1996. Role of uncoupled and non-coupled oxidations in maintenance of safely low levels of oxygen and its one-electron reductants. Q. Rev. Biophys. 29 (2), 169–202.
Starkov, A.A., Fiskum, G., 2003. Regulation of brain mitochondrial H_2O_2 production by membrane potential and NAD(P)H redox state. J. Neurochem. 86 (5), 1101–1107.
Umamaheswari, S., Priyadarshinee, S., Kadirvelu, K., Ramesh, M., 2021. Polystyrene microplastics induce apoptosis via ROS-mediated p53 signaling pathway in zebrafish. Chem. Biol. Interact. 345, 109550.
Van Acker, E., De Rijcke, M., Asselman, J., Beck, I.M., Huysman, S., Vanhaecke, L., De Schamphelaere, K.A.C., Janssen, C.R., 2020. Aerosolizable marine phycotoxins and human health effects: in vitro support for the biogenics hypothesis. Mar. Drugs 18 (1).
Van Cauwenberghe, L., Janssen, C.R., 2014. Microplastics in bivalves cultured for human consumption. Environ. Pollut. 193, 65–70.
Visalli, G., Facciolà, A., Pruiti Ciarello, M., De Marco, G., Maisano, M., Di Pietro, A., 2021. Acute and sub-chronic effects of microplastics (3 and 10 μm) on the human intestinal cells HT-29. Int. J. Environ. Res. Publ. Health 18 (11).
Wang, H., Shi, X., Gao, Y., Zhang, X., Zhao, H., Wang, L., Zhang, X., Chen, R., 2022. Polystyrene nanoplastics induce profound metabolic shift in human cells as revealed by integrated proteomic and metabolomic analysis. Environ. Int. 166, 107349.
Wang, Y., Wei, Z., Xu, K., Wang, X., Gao, X., Han, Q., Wang, S., Chen, M., 2023. The effect and a mechanistic evaluation of polystyrene nanoplastics on a mouse model of type 2 diabetes. Food Chem. Toxicol. 173, 113642.
Wei, Z., Wang, Y., Wang, S., Xie, J., Han, Q., Chen, M., 2022. Comparing the effects of polystyrene microplastics exposure on reproduction and fertility in male and female mice. Toxicology 465, 153059.
Wu, B., Wu, X., Liu, S., Wang, Z., Chen, L., 2019. Size-dependent effects of polystyrene microplastics on cytotoxicity and efflux pump inhibition in human Caco-2 cells. Chemosphere 221, 333–341.
Wu, T., Grootaert, C., Voorspoels, S., Jacobs, G., Pitart, J., Kamiloglu, S., Possemiers, S., Heinonen, M., Kardum, N., Glibetic, M., Smagghe, G., Raes, K., Van Camp, J., 2017. Aronia (Aronia melanocarpa) phenolics bioavailability in a combined in vitro digestion/Caco-2 cell model is structure and colon region dependent. J. Funct.Foods 38, 128–139.
Xi, W.-S., Song, Z.-M., Chen, Z., Chen, N., Yan, G.-H., Gao, Y., Cao, A., Liu, Y., Wang, H., 2019. Short-term and long-term toxicological effects of vanadium dioxide nanoparticles on A549 cells. Environ. Sci.: Nano 6 (2), 565–579.
Xie, X., Deng, T., Duan, J., Xie, J., Yuan, J., Chen, M., 2020. Exposure to polystyrene microplastics causes reproductive toxicity through oxidative stress and activation of the p38 MAPK signaling pathway. Ecotoxicol. Environ. Saf. 190, 110133.
Xu, M., Halimu, G., Zhang, Q., Song, Y., Fu, X., Li, Y., Li, Y., Zhang, H., 2019. Internalization and toxicity: a preliminary study of effects of nanoplastic particles on human lung epithelial cell. Sci. Total Environ. 694, 133794.
Yang, D., Shi, H., Li, L., Li, J., Jabeen, K., Kolandhasamy, P., 2015. Microplastic pollution in table salts from China. Environ. Sci. Technol. 49 (22), 13622–13627.
Ye, X.-Q., Li, Q., Wang, G.-H., Sun, F.-F., Huang, G.-J., Bian, X.-W., Yu, S.-C., Qian, G.-S., 2011. Mitochondrial and energy metabolism-related properties as novel indicators of lung cancer stem cells. Int. J. Cancer 129 (4), 820–831.
Zarus, G.M., Muianga, C., Hunter, C.M., Pappas, R.S., 2021. A review of data for quantifying human exposures to micro and nanoplastics and potential health risks. Sci. Total Environ. 756, 144010.
Zorova, L.D., Popkov, V.A., Plotnikov, E.Y., Silachev, D.N., Pevzner, I.B., Jankauskas, S. S., Babenko, V.A., Zorov, S.D., Balakireva, A.V., Juhaszova, M., Sollott, S.J., Zorov, D.B., 2018. Mitochondrial membrane potential. Anal. Biochem. 552, 50–59.